

Received: 2017.09.18  
Accepted: 2018.01.03  
Published: 2018.06.14

# Whey Acidic Protein/Four-Disulfide Core Domain 21 Regulate Sepsis Pathogenesis in a Mouse Model and a Macrophage Cell Line via the Stat3/Toll-Like Receptor 4 (TLR4) Signaling Pathway

Authors' Contribution:

Study Design A  
Data Collection B  
Statistical Analysis C  
Data Interpretation D  
Manuscript Preparation E  
Literature Search F  
Funds Collection G

AEF **Zhixiang Xie**  
BC **Zhuangbo Guo**  
DF **Jianfeng Liu**

Department of Emergency Medicine, Guangzhou Red Cross Hospital, Guangzhou, Guangdong, P.R. China

**Corresponding Author:** Zhixiang Xie, e-mail: 13929555313@163.com  
**Source of support:** Departmental sources

**Background:** Whey acidic protein/four-disulfide core domain 21 (Wfdc21), also known as Lnc-DC, it has been reported to be correlated with immune response. However, the role of Wfdc21 in the pathogenesis of sepsis is still unknown. In the present study, we aimed to investigate the role of Wfdc21 in the pathogenesis of sepsis.

**Material/Methods:** The cecal ligation and puncture (CLP)-induced sepsis model was established in Balb/c mice. Animals were euthanized 4, 8, 16, or 24 h after CLP. The glycogen distribution in the kidney and liver was checked by Periodic acid-Schiff (PAS) staining. Changes in the serum interleukin-1 $\beta$  (IL-1 $\beta$ ) and tumor necrosis factor- $\alpha$  (TNF- $\alpha$ ) concentrations were monitored with ELISA, and Wfdc21 expression was determined by qPCR. Mouse macrophage-like RAW264.7 cells were treated with different doses of lipopolysaccharide (LPS) from *Escherichia coli* to mimic sepsis *in vitro*. Western blot analysis was performed to confirm whether LPS-induced *in vitro* sepsis was correlated with the involvement of the Stat3/TLR4 signaling pathway. In addition, RAW 264.7 cells were infected with lentiviruses containing Wfdc21 shRNA to further confirm the role of Wfdc21 in the pathogenesis of sepsis.

**Results:** We found that Wfdc21 level was elevated in the CLP-induced animal model and LPS-treated RAW264.7 cells. Furthermore, the downregulation of Wfdc21 modulated the concentration of pro-inflammatory factors in LPS-treated macrophages, such as IL-1 $\beta$  and TNF- $\alpha$ , in LPS-treated macrophages. This regulatory effect was mediated through the Stat3/TLR4 signaling pathway, since Wfdc21 can regulate p-Stat3 and TLR4 levels in LPS-treated macrophages.

**Conclusions:** Wfdc21 plays a critical role in the pathogenesis of sepsis and may provide a therapeutic target for sepsis treatment.

**MeSH Keywords:** **Sepsis • STAT3 Transcription Factor • Toll-Like Receptor 4**

**Full-text PDF:** <https://www.medscimonit.com/abstract/index/idArt/907176>

 3611

 —

 6

 46



## Background

Sepsis is the primary cause of death in intensive care units (ICUs) and leads to substantially decreased quality of life in surviving patients [1]. The morbidity caused by sepsis reaches around 50–95 cases per 100 000 people in the USA annually [2], leading to high average mortality rates: 41% in Europe and 28% in the USA [3]. Current management of sepsis includes eradication of the infection source with use of appropriate antimicrobial treatment, together with aggressive supportive care or pulmonary therapy [4]. Despite the progress made in sepsis management and treatment, lack of understanding of the pathogenesis of sepsis hinders success in developing specific anti-sepsis medicines. In the mouse cecal ligation and puncture (CLP) model, some key proteins have been identified to be critical in sepsis pathogenesis, such as interleukins [5] and Toll-like receptors (TLR) [6]. All these proteins are correlated with the expression of pro-inflammatory cytokines and cell adhesion molecules [7]. Therefore, these proteins may serve as therapeutic targets in sepsis treatment.

WAP four-disulfide core domain 21 (Wfdc21) is one of the long non-coding RNAs (lncRNAs), which are regulatory RNAs longer than 200 nt and without protein-coding function. Wfdc21, also known as lnc-DC, is specifically expressed in dendritic cells [8]. There have been few studies on Wfdc21. The other member of the whey acidic protein/four-disulfide core (WAP/4-DSC) family, called Wdm1, was characterized as a differentiation-dependent gene in white and brown adipogenesis and a new adipokine, functioning in activation of matrix metalloproteinase-2 (MMP-2) [9], an enzyme that can catalyze the degradation of collagen and extracellular matrix [10]. WAP/4-DSC also plays roles in respiratory health and disease [11]. Wfdc family members are critical in occurrence of inflammation. In the lungs, Wfdc12 regulates the inflammatory response [12]. Wfdc1 is a key modulator of inflammatory and wound repair responses. Wfdc1 modulates inflammatory responses in wound repair [13]. Wfdc21 controls human dendritic cell differentiation through Stat3 signaling [8]. It also induces the over-maturation of dendritic cells in preeclampsia patients [14]. Functionally, Wfdc1 is likely to be established as a biomarker for systemic lupus erythematosus [15]. All these findings suggest that Wfdc family members can regulate the immune system and modulate the inflammatory response. Since sepsis is a dysregulated host response to infection, mainly mediated by the inflammatory response, we hypothesize that Wfdc family members are likely to play important roles in sepsis pathogenesis.

In the present study, we demonstrated the role of Wfdc21 in sepsis progression using a CLP-induced animal model and a cell-based model.

## Material and Methods

### Sepsis model

Thirty-two Balb/c mice, age 6 weeks, of Specific Pathogen-Free (SPF) grade, (weighing 20–25 g, female-to-male ratio 1: 1) were purchased from the Experimental Animal Center of Sun Yat-sen University (Guangzhou, China). The use of animals in this study was approved by the Animal Care Committee of Guangzhou Red Cross Hospital (Guangzhou, China). Cecal ligation and puncture (CLP) is a widely used experimental model of sepsis, which closely mimics the clinical symptom of sepsis, and CLP models exhibiting polymicrobial sepsis are considered as the criterion standard in sepsis research [16]. The CLP-induced sepsis model was developed as previously described [17]. In brief, after an overnight fast, mice were anesthetized using intraperitoneal injection of 30 mg/kg pentobarbital. A 1.5-cm midline incision was made on the anterior abdomen. The cecum was carefully isolated and the distal 1 cm was ligated. Then, the cecum was punctured once with a sterile 18-gauge needle, and was squeezed to extrude the cecal contents from the wounds. The cecum was repositioned and the abdomen was closed. Mice in the sham control group (n=2) underwent the same surgery, and the cecum was manipulated without being ligated or perforated. All mice were administered saline (2 ml/100 g body weight) subcutaneously immediately after surgery for fluid resuscitation. Two mg/kg buprenorphine was administered via intraperitoneal injection to relieve pain, and 10 mg/kg antibiotic (amoxicillin sodium) was administered by intraperitoneal injection after the surgery to prevent infection. Animals were euthanized at 0, 4, 8, 16, or 24 h (n=6/group) after CLP surgery. Peripheral blood was collected and centrifuged at 3500×g for 10 min at 4°C, and the supernatant serum was collected and stored at –20°C for further analysis. The kidneys and liver were dissected and stored in liquid nitrogen for further analysis.

### Cell culture

The mouse macrophage-like cell line RAW 264.7 was purchased from the American Type Culture Collection (ATCC, Manassas, VA). Cells were maintained in Dulbecco's modified Eagle's medium (DMEM) with 10% fetal bovine serum (FBS) at 37°C in a 5% CO<sub>2</sub> incubator. All the medium components were purchased from Thermo Fisher (Sunnyvale, CA, USA). Lipopolysaccharide (LPS)-stimulated macrophages are a widely used model of sepsis *in vitro* [18]. Therefore, in the present study we used the LPS-stimulated RAW264.7 to mimic sepsis *in vitro*. The cells were treated with different doses (1, 10, 50, or 100 ng/ml) of lipopolysaccharide (from *Escherichia coli* 055: B5, Cat. No. L2880, Sigma-Aldrich) for 4, 8, 16, or 24 h.

### Periodic acid-Schiff (PAS) staining

PAS staining was used to assess the glycogen content in the kidneys and liver of sepsis mice. The procedure of PAS was carried out as described previously [19]. Briefly, the kidney and liver tissue sections were deparaffinized in xylene, hydrated in graded ethanol, and then fixed in methyl Carnoy's solution, followed by washing 3 times with phosphate-buffered saline (PBS). Sections were then incubated with 0.5% periodic acid, washed in PBS, and stained with Schiff's reagent. Images were acquired using an Eclipse 90i microscope at 200× magnification (Nikon, Tokyo, Japan) equipped with a DP71 CCD camera image capture system (Olympus, Tokyo, Japan). The images were analyzed using Image-Pro Plus version 6.1, and glycogen content of each tissue is expressed as a percentage of the area that stained positive glycogen (% Area PAS<sup>+</sup>).

### Enzyme-linked immunosorbent assay (ELISA)

To confirm that sepsis was established in mice, we assessed serum IL-6 and IL-10 at 4 and 8 h after CLP or sham surgery by using ELISA kits (Cat. No. EK0411 and 0417; Boster Biological Technology Co. Ltd., Wuhan, China). The serum samples or cell samples were collected at different time points after CLP surgery or LPS treatment. Serum IL-1 $\beta$  and TNF- $\alpha$  concentration change among different groups was monitored by ELISA. After coating, plates were sequentially washed with PBST buffer and blocked with 1% BSA and incubated for 1 h at 37°C. Then, anti-IL-1 $\beta$  (Cat. No. EK0394) or TNF- $\alpha$  antibody (Cat. No. EK0527) (Boster Biological Technology Co. Ltd, Wuhan, China) and HRP-conjugated antibody were sequentially added and incubated for 1 h at 37°C. The detection was achieved by adding chromogenic substrate, 3,3',5,5'-Tetramethylbenzidine (TMB). Absorbance was measured at 450 nm with an EnSpire multi-mode plate reader (Perkin Elmer, Waltham, MA).

### RNA extraction and qPCR

Total RNA extraction was performed using TRIzol reagent (Life Technologies) according to the manufacturer's instruction. Two micrograms of total RNA extracted from the cells was subjected to reverse transcription (RT). Synthesis of cDNA was performed by using the one-step RT-PCR kit from Takara. SYBR Green (Toyobo) RT-PCR amplification and real-time fluorescence detection were performed using an ABI 7300 real-time PCR thermal cycle instrument (ABI, USA), according to the supplied protocol. Primers used were: Wfdc21-F: GTTGGTGTCCTCATCACCC, Wfdc21-R: CACAGGTGCCTAAAGCTGC;  $\beta$ -Actin-F: GGCTGATCCCTCCATCG,  $\beta$ -Actin-R: CCAGTTGGTAACAATGCCATGT. Each PCR reaction contained 20  $\mu$ l solution, including cDNA template, primers, and SYBR green mix. The protocol was: 3 min at 98°C followed by

30 cycles, including 15 s at 98°C, 15 s at 55°C, and 30 s at 72°C. Relative gene expression was calculated by the 2<sup>- $\Delta\Delta$ Ct</sup> method.

### Western blotting

For protein extraction, cultured cells were first lysed in cell lysis buffer, the cell lysate was centrifuged at 10 000×g for 10 min at 4°C, and the clear supernatant was collected. After determination of protein concentrations by the BCA method, 100- $\mu$ g protein samples were loaded on each lane of 10% polyacrylamide gel, and then blotted onto a polyvinylidene difluoride (PVDF) membrane. After blocking with PBST containing 5% nonfat dry milk, the membrane was incubated with antibodies against TLR4 (Santa Cruz, sc-293072, 1: 500), P-Stat3 (Cell Signaling Technologies, cst9145, 1: 1000), Stat3 (Cell Signaling Technologies, cst9139, 1: 1000), and GAPDH (Transgen, HC301, 1: 8000). Peroxidase-linked anti-rabbit IgG (Life Technologies, USA) was used as secondary antibody. These proteins were visualized by using an ECL Western blotting detection kit (Amersham Biosciences) and were analyzed by ImageJ software version 1.48 (NIH, MD, USA).

### Wfdc21 knockdown by RNA interference

The genetic sequence of Wfdc21 was obtained from GenBank ([https://www.ncbi.nlm.nih.gov/nucleotide/NC\\_000077.6?report=genbank&from=83746940&to=83752646](https://www.ncbi.nlm.nih.gov/nucleotide/NC_000077.6?report=genbank&from=83746940&to=83752646)). Short hairpin RNA (shRNA) targeting Wfdc21 and a scrambled sequence serving as control were cloned into the lentiviral vector with 2 other plasmids coding for the lentiviral envelope (pCMV-VSV-G) and packaging proteins (pCMV delta R8.2). The sequence of shWfdc21 was GTTAACTGTCATGAAGCTAGGAGCCTTTCAAGAGAAAGGCTCCTAGCTTCATGCTTTTTTCTCCTCGAG. Those constructs were co-transfected into 293T cells using Lipofectamine 2000 (Life Technologies, USA) and viral particles were collected 48 h later as described previously [20]. RAW 264.7 cells were infected with lentiviruses containing Wfdc21 shRNA or scrambled sequence for 24 h.

### Statistical analysis

The concentration of in ELISA was calculated by the standard curve derived from the standard sample provided in ELISA kit. The value of grey area in Western blot data was analyzed by Image J software version 1.48. Data are presented as mean value + standard deviation (SD). Statistical analysis was performed using the Mann-Whitney U test for pooled data from 3 independent experiments. Unpaired, 2-tailed Student's *t* tests or one-way ANOVA were used to determine significant differences. A *p* value less than 0.05 was considered as significantly different.

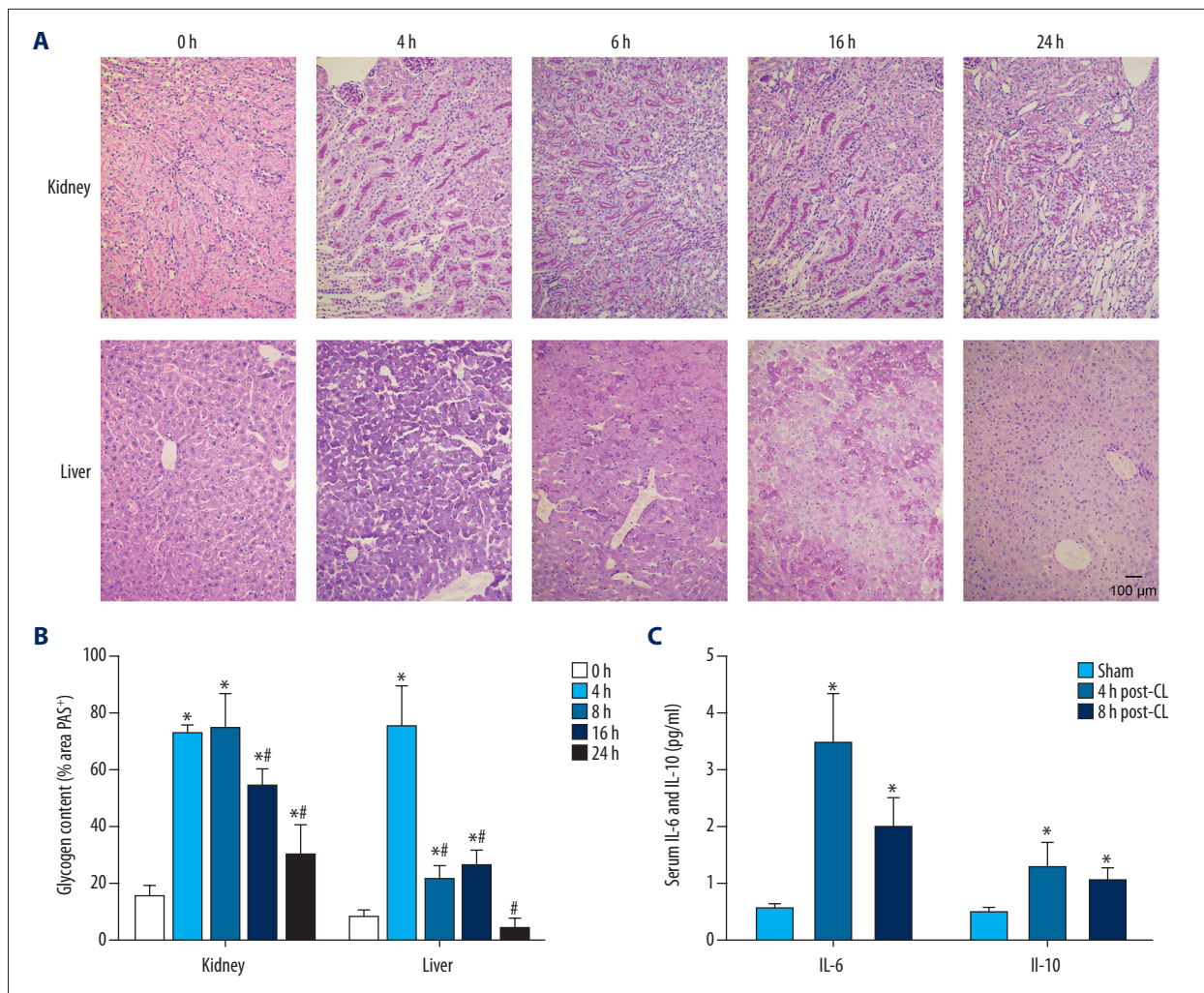


**Figure 1.** (A) Glycogen distribution in the kidneys and liver of the CLP-induced mouse model by PAS staining. Compared to untreated control (0 h), glycogen aggregation occurred in the sepsis model at various durations (4, 8, 16, and 24 h) in kidneys and liver. Scale bar: 100  $\mu$ m. (B) PAS staining images were analyzed using Image-Pro Plus version 6.1, and glycogen content of each tissue is expressed as a percentage of the area that stained positive for glycogen (% Area PAS<sup>+</sup>). \*  $P < 0.05$  vs. 0 h, #  $P < 0.05$  vs. 4 h. (C) Serum IL-6 and IL-10 at 4 and 8 h after CLP or sham surgery were measured using ELISA kits. \*  $P < 0.05$  vs. sham group.

## Results

### Abnormal glycogen distribution in the CLP-induced sepsis model

To confirm the successful establishment of the CLP-induced sepsis model, we assessed the glycogen distribution in kidney and liver by Periodic acid–Schiff (PAS) stain. The glycogen was stained by PAS and observed as red and the nuclei were observed as blue. The area of glycogen PAS staining was measured by image analysis using Image-Pro Plus. The data indicated that glycogen was evenly distributed in liver and kidneys of control animals without the CLP surgery (Figure 1A, 1B), but glycogen aggregation appeared in the kidneys and liver in the

sepsis model at 4 h after CLP (Figure 1A, 1B), and this aggregation appears to be gradually weakened with prolonged CLP surgery (Figure 1A, 1B). Therefore, these data show that glycogen distribution in kidneys and liver is affected by CLP, demonstrating the establishment of the sepsis model.

### Elevated IL-6, IL-10, and IL-1 $\beta$ /TNF- $\alpha$ concentrations and Wfdc21 level in the sepsis model

To further validate sepsis model establishment, we assessed the alteration in serum IL-6 and IL-10 levels. Induction of pro-inflammatory and anti-inflammatory cytokines, such as IL-6 and IL-10, has been documented in sepsis [21]. We found that pro-inflammatory IL-6 and anti-inflammatory IL-10 were

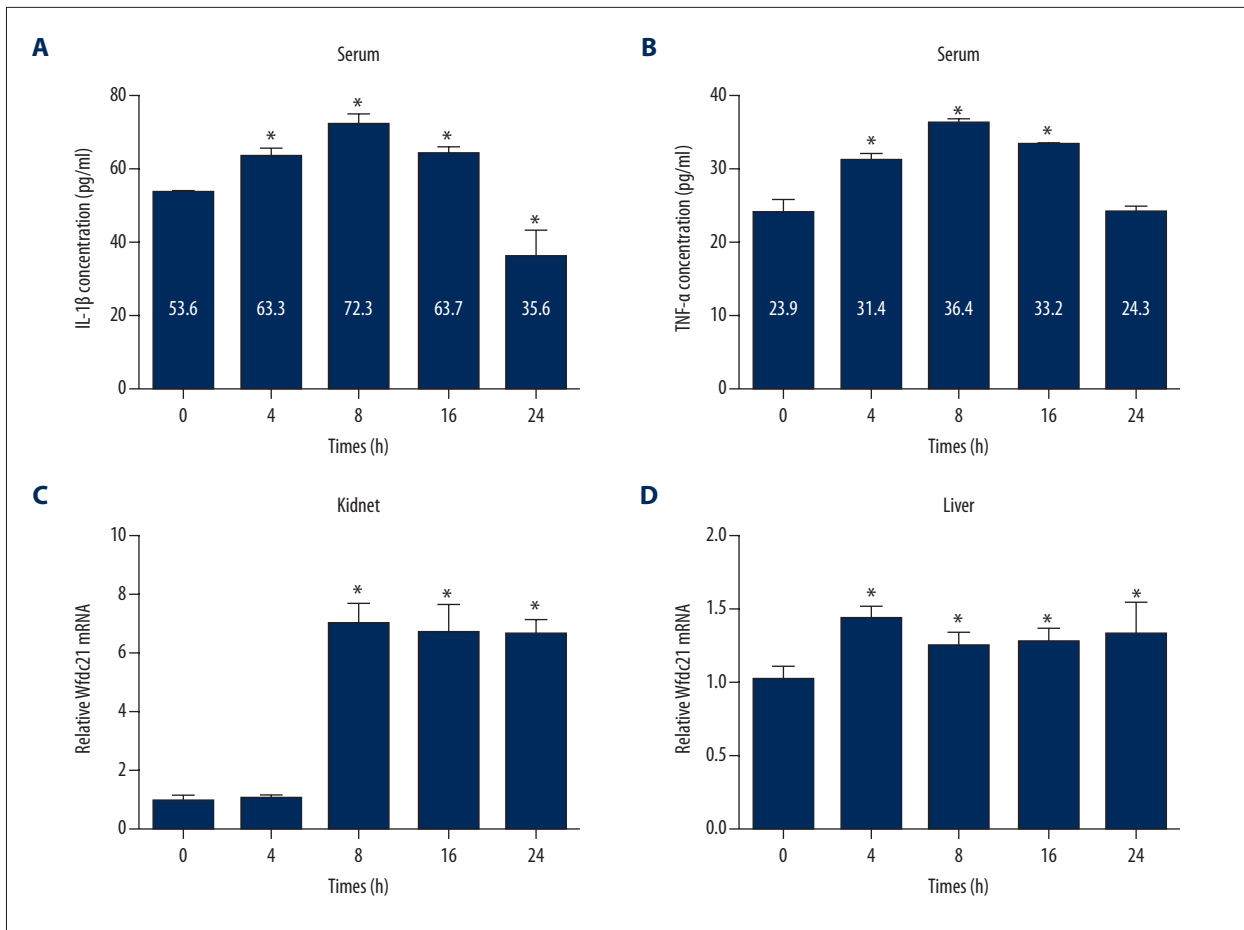


**Figure 2.** Concentrations of inflammatory factors (IL-1 $\beta$  and TNF- $\alpha$ ) and Wfdc21 mRNA expression were altered in the sepsis model. Serum IL-1 $\beta$  (A) and TNF- $\alpha$  (B) concentrations were elevated in the CLP-induced sepsis model. Wfdc21 mRNA level was increased in the sepsis model in both kidneys (C) and liver (D). \*  $P < 0.05$  vs. 0 h.

significantly increased in CLP animals compared to sham animals at 4 h and 8 h after surgery (Figure 1C). In addition, the dynamic changes in serum IL-1 $\beta$  and TNF- $\alpha$  levels at 0, 4, 8, 16, and 24 h after CLP surgery was measured. The ELISA data demonstrated that both IL-1 $\beta$  and TNF- $\alpha$  concentrations were significantly increased at 4 h and reached the maximum at 8 h after CLP surgery (Figure 2A, 2B). Then, the IL-1 $\beta$  and TNF- $\alpha$  concentrations decreased at 16 and 24 h after CLP surgery (Figure 2A, 2B). However, the IL-1 $\beta$  and TNF- $\alpha$  concentrations at 16 h after CLP surgery were still higher than in the control animals (Figure 2A, 2B), while the IL-1 $\beta$  concentration at 24 h after CLP surgery was lower than in the control animals (Figure 2A). In kidneys, the Wfdc21 mRNA level was increased at 8, 16, and 24 h after CLP surgery (Figure 2C), while the Wfdc21 mRNA level was significantly increased at all 4 time points (4, 8, 16, and 24 h) in liver (Figure 2D). IL-6, IL-10, IL-1 $\beta$ , and TNF- $\alpha$  concentrations in serum, as well as Wfdc21 level in liver and kidneys, was elevated in the sepsis model.

#### LPS increased the IL-1 $\beta$ /TNF- $\alpha$ concentrations and Wfdc21 level in RAW264.7 cells

To confirm the role of Wfdc21 in the pathogenesis of sepsis, mouse macrophages line RAW264.7 cells was treated with LPS to mimic the sepsis progression *in vitro*. The ELISA data indicated that the IL-1 $\beta$  and TNF- $\alpha$  concentrations in supernatants reached the highest level at 8 h after 1-ng/ml LPS treatment (Figure 3A, 3B). At 4 and 8 h after 10-ng/ml LPS treatment, the IL-1 $\beta$  concentration was significantly higher than in the untreated group (Figure 3A). However, the increase in IL-1 $\beta$  concentration was not present when the LPS treatment duration was extended to 16 or 24 h, or when 50 and 100 ng/ml LPS was used (Figure 3A). By contrast, the change in TNF- $\alpha$  concentration was more obvious, since all 4 doses of LPS significantly increased TNF- $\alpha$  concentration at various exposure times (Figure 3B). Similarly, all 4 concentrations of LPS increased Wfdc21 mRNA level at 8 h after stimulation (Figure 3C). These data demonstrate that Wfdc21 expression level and

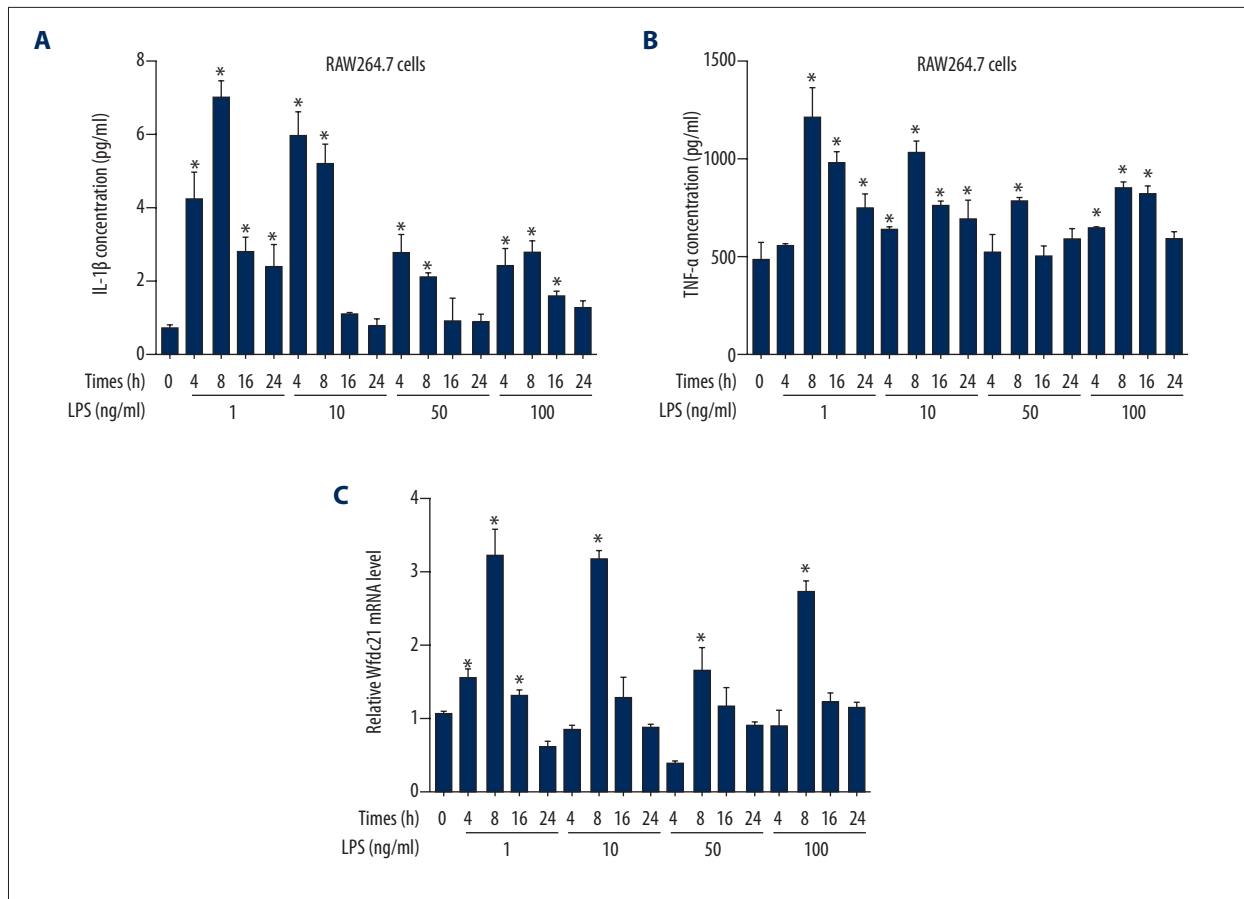


**Figure 3.** LPS stimulation changed concentrations of inflammatory factors (IL-1 $\beta$  and TNF- $\alpha$ ) and Wfdc21 mRNA level in RAW264.7 cells. IL-1 $\beta$  (A) and TNF- $\alpha$  (B) concentration was increased in LPS-treated cells at various time points. (C) Wfdc21 mRNA level was elevated at different times after LPS treatment. \*  $P < 0.05$  vs. (0 h, 0 ng/ml LPS).

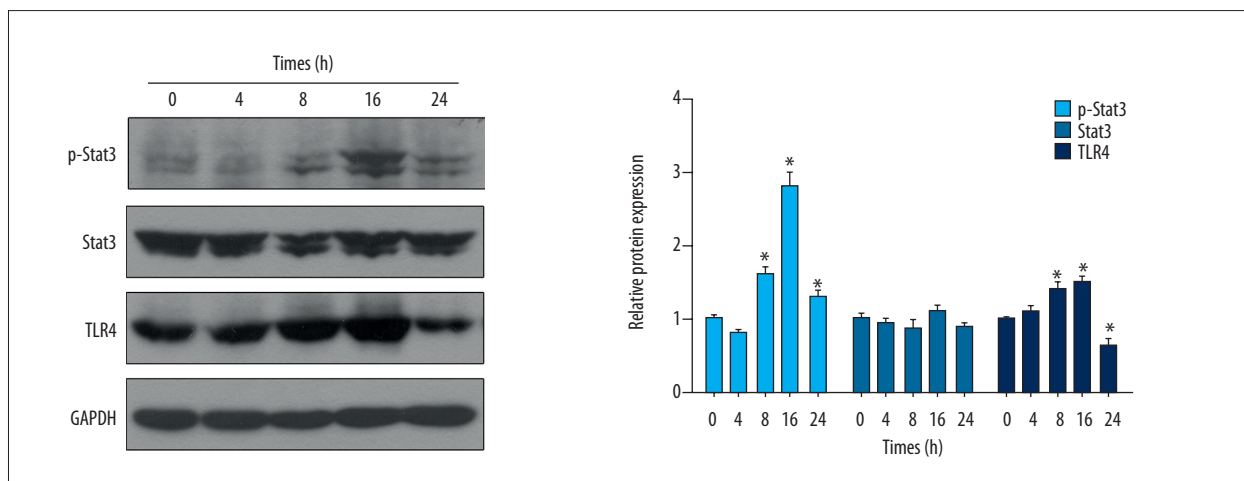


**Figure 4.** LPS led to the alteration in Stat3/TLR4 signaling. Western blotting assay showed the increase in p-Stat3 and TLR4 level with stimulation of LPS in RAW264.7 cells, and the statistical analysis is shown. \*  $P < 0.05$  vs. 0 h.

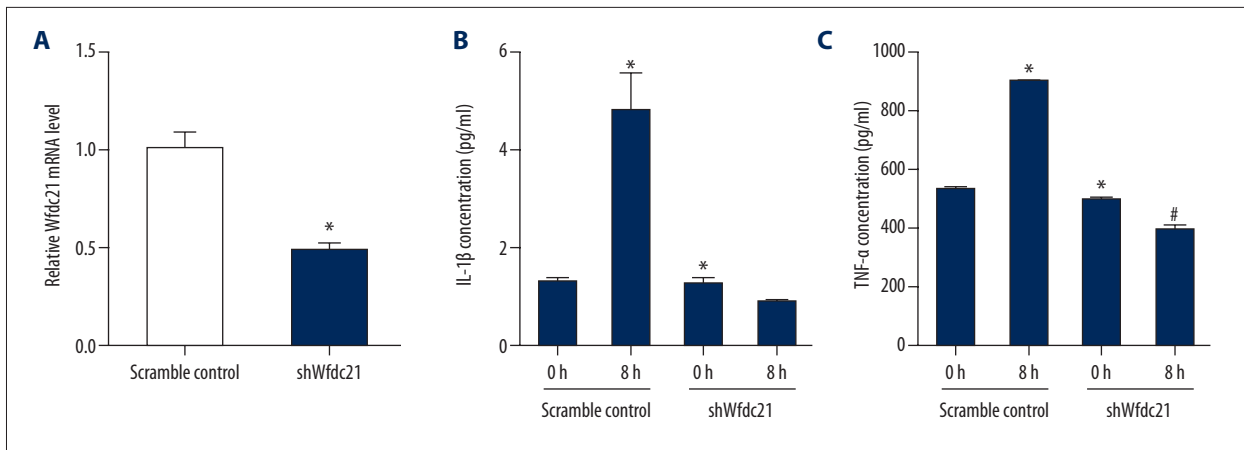


**Figure 5.** Wfdc21 regulated the concentrations of inflammatory factors with the LPS treatment. (A) The Wfdc21 mRNA level was decreased in shWfdc21-transfected RAW264.7 cells. IL-1 $\beta$  (B) or TNF- $\alpha$  (C) concentration was not significantly increased in LPS-treated RAW264.7 cells transfected with shWfdc21. \*  $P < 0.05$  compared to the scramble control cells; #  $P < 0.05$  compared to the untreated shWfdc21-transfected cells.

pro-inflammatory factors secretion are elevated in LPS-treated RAW264.7 cells at 8 h after stimulation.

#### LPS-induced sepsis in RAW264.7 cells activated the Stat3/TLR4 signaling pathway

Then, we assessed whether LPS-induced sepsis in *in vitro* was correlated with the activation of the Stat3/TLR4 signaling. Western blotting data indicated that the p-Stat3 level began to increase at 8 h after LPS stimulation, and the p-Stat3 level continued to increase at 16 h and decreased at 24 h after LPS stimulation (Figure 4). Similar results were obtained for the TLR4 level, showing increased TLR4 levels at 8 and 16 h, and decreased levels at 24 h after LPS stimulation (Figure 4). There appear to be 2 bands for Stat3 and for p-Stat3; because Stat3 has 2 subtypes (Stat3 $\alpha$  and Stat3 $\beta$ ), they are co-expressed in various cell types. The phosphorylation of Stat3 should be a rather quick event occurring in less than 8 h, unlike the transcription of TLR4; however, our Western blotting results showed the expression of p-Stat3 and TLR4 simultaneously, which indicated that the increase of p-Stat3 occurs immediately after upregulated expression of TLR4. This dynamic change in p-Stat3 and TLR4 levels after LPS stimulation demonstrates the involvement of Stat3/TLR4 signaling with the LPS stimulation in macrophages.

#### Downregulation of Wfdc21 decreased IL-1 $\beta$ and TNF- $\alpha$ concentrations in LPS-treated macrophages

Since LPS could change IL-1 $\beta$  and TNF- $\alpha$  as well as the Wfdc21 simultaneously, we assessed whether Wfdc21 regulates the IL-1 $\beta$  and TNF- $\alpha$  concentrations in LPS-treated macrophages. Wfdc21 mRNA level was significantly decreased in shWfdc21-transfected cells compared to the scramble control (Figure 5A).

Neither IL-1 $\beta$  nor TNF- $\alpha$  concentration was significantly increased by LPS stimulation when Wfdc21 was downregulated, while the scramble control transfected cells showed robust increases in IL-1 $\beta$  and TNF- $\alpha$  concentrations in the presence of LPS, and the knockdown of Wfdc21 showed a slight decrease in the secretion of IL-1 $\beta$  and a significant decrease in the expression of TNF- $\alpha$  (Figure 5B, 5C). These data show that Wfdc21 can regulate the IL-1 $\beta$  or TNF- $\alpha$  levels that were elevated by LPS stimulation.

#### Downregulation of Wfdc21 prevented the activation of the Stat3/TLR4 signaling pathway

Then, we determined if regulation of Wfdc21 controlled activation of the Stat3/TLR4 pathway. Wfdc21 downregulation led to the reduced level of p-Stat3 or TLR4 with or without the LPS treatment at 0 h (Figure 6). In shWfdc21-transfected cells, LPS significantly increased the p-Stat3 or TLR4 level at 16 h compared to shWfdc21-transfected cells at 0 h of LPS treatment (Figure 6). Therefore, it is possible that Wfdc21 can regulate the Stat3/TLR4 signaling pathway activated by LPS treatment.

## Discussion

It has been reported that Wfdc21 protein (Lnc-DC) affects the differentiation of monocytes into dendritic cells, as well as the T cell activation [8]. Therefore, it is reasonable to speculate that Wfdc21 plays a vital role in immune responses. In previous reports, sepsis resulted in the glycogen accumulation in multiple tissues, including lung [22], liver [23], and kidney [24]. Through an *in vitro* model, it was demonstrated that sepsis progression controls hepatic glycogen metabolism [25]. Patients with sepsis are characterized by disordered energy metabolism, such

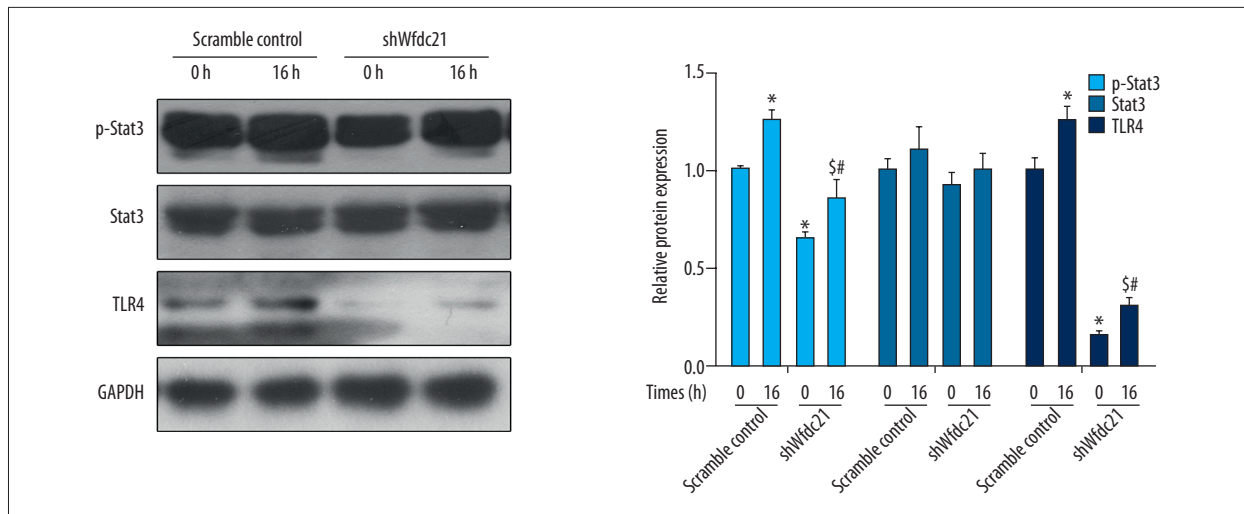


**Figure 6.** LPS-induced increase in p-Stat3 or TLR4 level was counteracted by downregulation of Wfdc21. The p-Stat3 or TLR4 level was reduced with shWfdc21-transfection in LPS-treated cells, compared to the scramble control cells, and the statistical analysis is shown. \*  $P < 0.05$  compared to the scramble control cells; #  $P < 0.05$  compared to the scramble control cells treated with LPS for 16 h; \$  $P < 0.05$  compared to the untreated shWfdc21-transfected cells.

as increased protein decomposition, glycogen accumulation, and fat mobilization, and these metabolic changes can serve as biomarkers for sepsis severity [26]. In addition, sepsis-induced liver glycogen accumulation can cause reduced food intake and induce insulin resistance [27]. A major feature of the progression of sepsis is failure to regulate glucose homeostasis [28]. The kidneys and liver have been found to participate in the synthesis and accumulation of glycogen during the progression of sepsis [29,30]. Several studies have attributed the alteration of glycogen stores to changes in the activities of glycogen synthase [31,32], and glucose metabolic disorder is mediated by inflammatory cytokines such as IL-1, IL-6, and TNF- $\alpha$  [33]. These cytokines can have direct effects on hepatocytes or alter the expression levels of glycol-regulatory hormones.

In this study, we investigated the function of Wfdc21 in sepsis pathogenesis. We found that Wfdc21 level was elevated in sepsis models, and regulation of this gene controls the secretion of IL-1 $\beta$  and TNF- $\alpha$  induced by LPS stimulation in macrophages. The Stat3/TLR4 signaling pathway was mediated by Wfdc21 in LPS-treated macrophages. Therefore, we hypothesized that Wfdc21 is critical in sepsis occurrence and may serve as a potential target in therapy against sepsis. Our findings demonstrated the glycogen accumulation was enhanced in the liver and kidneys in a CLP-induced sepsis model, furthering proving the potential sepsis pathogenesis in term of glycogen metabolism. In addition, we found that the downregulation of Wfdc21 controls the secretion of pro-inflammatory factors induced by the LPS stimulation in macrophages. In previous studies, it has been reported that TNF- $\alpha$  and IL-1 $\beta$  mRNA was rapidly induced by LPS stimulation, and that macrophages secrete numerous pro-inflammatory cytokines,

including TNF- $\alpha$  and IL-1 $\beta$ , in order to mediate the inflammatory response [34,35]. Unexpectedly, our results revealed that TNF- $\alpha$  and IL-1 $\beta$  secretion is independent of the LPS concentration, and Wfdc21 expression is also independent of the LPS concentration. It appears that, unlike IL-1 $\beta$ , TNF- $\alpha$  is constitutively active even in untreated cells. Beutler et al. [35] have shown that regulation of TNF- $\alpha$  expression in macrophages exposed to LPS occurs post-transcriptionally, indicating that its accumulation is due mainly to post-transcriptional stabilization. We predict that in macrophages, TNF- $\alpha$  and IL-1 $\beta$  are regulated by Wfdc21 transcriptional activity. It will be important to determine the mechanisms whereby LPS-induced TNF- $\alpha$  and IL-1 $\beta$  secretion is modulated by Wfdc21 expression in further research. Macrophages are differentiated from circulating monocytes through the induction of local growth factors, including pro-inflammatory cytokines [36]. Therefore, Wfdc21 may inhibit the secretion of IL-1 $\beta$  and TNF- $\alpha$  in LPS-treated macrophages through controlling the differentiation of monocytes. IL-1 $\beta$  and TNF- $\alpha$  are 2 of the main pro-inflammatory factors, which are critical in inflammation and are key factors in evaluating sepsis progression [37,38]. We found the knockdown of Wfdc21 caused a slight decrease in IL-1 $\beta$  and TNF- $\alpha$  levels. shWfdc21 also significantly increased the p-Stat3 or TLR4 level at 16 h. These data suggest that the Stat3/TLR4 signaling pathway is involved in the regulation of Wfdc21-controlled secretion of IL-1 $\beta$  and TNF- $\alpha$ . The downstream mediators of the Stat3/TLR4 signaling pathway are still unknown; prime candidates are the pro-inflammatory cytokines (IL-1 $\beta$  and TNF- $\alpha$ ), increased gene expression and production of these cytokines, most probably mediated by the transcription factor NF $\kappa$ B, which have been demonstrated in previous studies [39,40]. Our data showing that regulation of Wfdc21 altered IL-1 $\beta$  and TNF- $\alpha$

concentration lead us to conclude that Wfdc21 plays a critical role in modulating sepsis progression through affecting pro-inflammatory factors.

Based on the LPS-stimulated-macrophages model, we demonstrated that the effect of Wfdc21 on pro-inflammatory factors secretion in LPS-treated macrophages was likely to be mediated by Stat3/TLR4 signaling. This is consistent with the finding that Wfdc1 promote the phosphorylation of tyrosine-705 of Stat3 by binding to Stat3, thus affecting the transcription of downstream genes [8]. Therefore, probing the downstream signaling will be a potential future research direction. Engagement of TLR4 induces the TRIF-dependent signaling pathway, leading to the production of interferon (IFN)- $\beta$  [41], which is critically regulated by NF- $\kappa$ B signaling [42]. This is a potential underlying mechanism of the effect of Wfdc21 regulation on sepsis progression, since the presence of Wfdc21 expression can induce inflammation, and this process is probably counteracted by inhibiting the proliferation of macrophages. Stat3 is a major signaling molecule that regulates the inflammatory activities of various cell types [43]. Phosphorylation of Stat3 is a critical step in sepsis pathogenesis [44]. TLR4 is recognized as an innate immunity receptors, the activation of TLRs results in the induction of the genes involved in antimicrobial activity [45]. In the present study, knockdown of Wfdc21 was shown to immediately decrease the expression of TLR4 at 0 h, which suggests that Wfdc21 positively regulates the expression of TLR4 protein. LPS is an agonist for Toll-like receptor (TLR) 4

and expresses many genes, including NF- $\kappa$ B and interferon regulatory factor (IRF)-3/IFN-inducible genes in macrophages and dendritic cells (DCs) [46]. After 16 h of LPS treatment, TLR-4 showed a slight increase, indicating that it is essential for the activation of the immune response induced by LPS. It has been reported that activation of TLR4 by its principal agonist, LPS, results in an immunostimulatory intracellular signaling pathway leading to the activation of the transcriptional factor, NF $\kappa$ B [12]. Our data show that TLR4 expression was inhibited by shWfdc21, and then responded rapidly to LPS stimulation. Thus, it is important to determine how the downstream genes of the Stat3/TLR4 signaling pathway regulate the occurrence and progression of sepsis. Downstream genes such as Akt, ERK, and NF- $\kappa$ B need to be investigated further.

## Conclusions

In conclusion, our main findings are that Wfdc21 was upregulated in the sepsis models, Wfdc1 downregulation inhibited the secretion of pro-inflammatory factors, and the Stat3/TLR4 signaling pathway was involved in the process. Thus, these findings indicate that Wfdc21 plays a critical role in the pathogenesis of sepsis.

## Conflict of interest

None.

## References:

- Hotchkiss RS, Karl IE: The pathophysiology and treatment of sepsis. *N Engl J Med*, 2003; 348(2): 138–50
- Dombrovskiy VY, Martin AA, Sunderram J, Paz HL: Rapid increase in hospitalization and mortality rates for severe sepsis in the United States: A trend analysis from 1993 to 2003. *Crit Care Med*, 2007; 35(5): 1244–50
- Levy MM, Artigas A, Phillips GS et al: Outcomes of the surviving sepsis campaign in intensive care units in the USA and Europe: A prospective cohort study. *Lancet Infect Dis*, 2012; 12(12): 919–24
- Sharma VK, Dellinger RP: Treatment options for severe sepsis and septic shock. *Expert Rev Anti Infect Ther*, 2006; 4(3): 395–403
- Zhao HQ, Li WM, Lu ZQ et al: The growing spectrum of anti-inflammatory interleukins and their potential roles in the development of sepsis. *J Interferon Cytokine Res*, 2015; 35(4): 242–51
- Weighardt H, Holzmann B: Role of Toll-like receptor responses for sepsis pathogenesis. *Immunobiology*, 2007; 212(9–10): 715–22
- Ince C, Mik EG: Microcirculatory and mitochondrial hypoxia in sepsis, shock, and resuscitation. *J Appl Physiol* (1985), 2016; 120(2): 226–35
- Wang P, Xue YQ, Han YM et al: The STAT3-binding long noncoding RNA lnc-DC controls human dendritic cell differentiation. *Science*, 2014; 344(6181): 310–13
- Wu Y, Smas CM: Wdnm1-like, a new adipokine with a role in MMP-2 activation. *Am J Physiol Endocrinol Metab*, 2008; 295(1): E205–15
- Aimes RT, Quigley JP: Matrix metalloproteinase-2 is an interstitial collagenase. Inhibitor-free enzyme catalyzes the cleavage of collagen fibrils and soluble native type I collagen generating the specific 3/4- and 1/4-length fragments. *J Biol Chem*, 1995; 270(11): 5872–76
- Small DM, Doherty DF, Dougan CM et al: The role of whey acidic protein four-disulfide-core proteins in respiratory health and disease. *Biol Chem*, 2017; 398(4): 425–40
- Glasgow AM, Small DM, Scott A et al: A role for whey acidic protein four-disulfide-core 12 (WFDC12) in the regulation of the inflammatory response in the lung. *Thorax*, 2015; 70(5): 426–32
- Ressler SJ, Dang TD, Wu SM et al: WFDC1 Is a Key Modulator of Inflammatory and Wound Repair Responses. *Am J Pathol*, 2014; 184(11): 2951–64
- Zhang W, Zhou Y, Ding Y: Lnc-DC mediates the over-maturation of decidual dendritic cells and induces the increase in Th1 cells in preclampsia. *Am J Reprod Immunol*, 2017; 77(6): 10.1111/aji.12647
- Wu GC, Li J, Leng RX et al: Identification of long non-coding RNAs GAS5, linc0597 and lnc-DC in plasma as novel biomarkers for systemic lupus erythematosus. *Oncotarget*, 2017; 8(14): 23650–63
- Brooks HF, Osabutey CK, Moss RF et al: Caecal ligation and puncture in the rat mimics the pathophysiological changes in human sepsis and causes multi-organ dysfunction. *Metab Brain Dis*, 2007; 22(3–4): 353–73
- Hu Z, Gu Z, Sun M et al: Ursolic acid improves survival and attenuates lung injury in septic rats induced by cecal ligation and puncture. *J Surg Res*, 2015; 194(2): 528–36
- West MA, Koons A: Endotoxin tolerance in sepsis: concentration-dependent augmentation or inhibition of LPS-stimulated macrophage TNF secretion by LPS pretreatment. *J Trauma*, 2008; 65(4): 893–98
- Zhou X, Bai C, Sun X et al: Puerarin attenuates renal fibrosis by reducing oxidative stress induced-epithelial cell apoptosis via MAPK signal pathways *in vivo* and *in vitro*. *Ren Fail*, 2017; 39(1): 423–31
- Gao Y, Yao A, Zhang W et al: Human mesenchymal stem cells overexpressing pigment epithelium-derived factor inhibit hepatocellular carcinoma in nude mice. *Oncogene*, 2010; 29(19): 2784–94

21. Sikora JP, Chlebna-Sokol D, Krzyzanska-Oberbek A: Proinflammatory cytokines (IL-6, IL-8), cytokine inhibitors (IL-6sR, sTNFR1I) and anti-inflammatory cytokines (IL-10, IL-13) in the pathogenesis of sepsis in newborns and infants. *Arch Immunol Ther Exp*, 2001; 49(5): 399–404
22. Liu ZY, Bone N, Jiang SN et al: AMP-activated protein kinase and glycogen synthase kinase 3 beta modulate the severity of sepsis-induced lung injury. *Mol Med*, 2015; 21: 937–50
23. Jellestad L, Fink T, Pradarutti S et al: Inhibition of glycogen synthase kinase (GSK)-3-beta improves liver microcirculation and hepatocellular function after hemorrhagic shock. *Eur J Pharmacol*, 2014; 724: 175–84
24. Coldewey SM, Khan AI, Kapoor A et al: Erythropoietin attenuates acute kidney dysfunction in murine experimental sepsis by activation of the beta-common receptor. *Kidney Int*, 2013; 84(3): 482–90
25. Wallington J, Ning J, Titheradge MA: The control of hepatic glycogen metabolism in an *in vitro* model of sepsis. *Mol Cell Biochem*, 2008; 308(1–2): 183–92
26. Englert JA, Rogers AJ: Metabolism, metabolomics, and nutritional support of patients with sepsis. *Clin Chest Med*, 2016; 37(2): 321–31
27. Litherland GJ, Morris NJ, Walker M, Yeaman SJ: Role of glycogen content in insulin resistance in human muscle cells. *J Cell Physiol*, 2007; 211(2): 344–52
28. Wolfe RR, Burke JF: Glucose and lactate metabolism in experimental septic shock. *Am J Physiol*, 1978; 235(5): R219
29. Curnow RT, Rayfield EJ, George DT et al: Altered hepatic glycogen metabolism and glucoregulatory hormones during sepsis. *Am J Physiol*, 1976; 230(5): 1296–301
30. Deaciuc IV, Spitzer JA: Rat liver free cytosolic Ca<sup>2+</sup> and glycogen phosphorylase in endotoxemia and sepsis. *Am J Physiol*, 1986; 251(5 Pt 2): R984–95
31. Ardawi MS, Ashy AA, Jamal YS, Khoja SM: Metabolic control of hepatic gluconeogenesis in response to sepsis. *J Lab Clin Med*, 1989; 114(5): 579–86
32. Liu MS, Kang GF: Liver glycogen metabolism in endotoxin shock. II. Endotoxin administration increases glycogen phosphorylase activities in dog livers. *Biochem Med Metab Biol*, 1987; 37(1): 73–80
33. Tsiotou AG: Septic shock; Current pathogenetic concepts from a clinical perspective. *Med Science Monit*, 2006; 12(4): LE4
34. Lin WW, Karin M: A cytokine-mediated link between innate immunity, inflammation, and cancer. *J Clin Invest*, 2007; 117(5): 1175–83
35. Beutler B: Application of transcriptional and posttranscriptional reporter constructs to the analysis of tumor necrosis factor gene regulation. *Am J Med Sci*, 1992; 303(2): 129–33
36. Shi C, Pamer EG: Monocyte recruitment during infection and inflammation. *Nat Rev Immunol*, 2011; 11(11): 762–74
37. Zabrodskii PF, Gromov MS, Maslyakov VV: Combined effects of M1 muscarinic acetylcholine receptor agonist TBPB and alpha 7n-acetylcholine receptor activator GTS-21 on mouse mortality and blood concentration of proinflammatory cytokines in sepsis. *Bull Exp Biol Med*, 2017; 162(6): 750–53
38. Arslan MS, Basuguy E, Ibiloglu I et al: Effects of Ecballium elaterium on proinflammatory cytokines in a rat model of sepsis. *J Invest Surg*, 2016; 29(6): 399–404
39. Notebaert S, Demon D, Vanden Berghe T et al: Inflammatory mediators in *Escherichia coli*-induced mastitis in mice. *Comp Immunol Microbiol Infect Dis*, 2008; 31(6): 551–65
40. Yang W, Zerbe H, Petzl W et al: Bovine TLR2 and TLR4 properly transduce signals from *Staphylococcus aureus* and *E. coli*, but *S. aureus* fails to both activate NF-kappaB in mammary epithelial cells and to quickly induce TNFalpha and interleukin-8 (CXCL8) expression in the udder. *Mol Immunol*, 2008; 45(5): 1385–97
41. Hoebe K, Du X, Georgel P, Janssen E et al: Identification of Lps2 as a key transducer of MyD88-independent TIR signalling. *Nature*, 2003; 424(6950): 743–48
42. Han KJ, Su XQ, Xu LG et al: Mechanisms of the TRIF-induced interferon-stimulated response element and NF-kappa B activation and apoptosis pathways. *J Biol Chem*, 2004; 279(15): 15652–61
43. Yu H, Pardoll D, Jove R: STATs in cancer inflammation and immunity: A leading role for STAT3. *Nat Rev Cancer*, 2009; 9(11): 798–809
44. McClure C, McPeak MB, Youssef D et al: Stat3 and C/EBP beta synergize to induce miR-21 and miR-181b expression during sepsis. *Immunol Cell Biol*, 2017; 95(1): 42–55
45. Akira S, Takeda K, Kaisho T: Toll-like receptors: Critical proteins linking innate and acquired immunity. *Nat Immunol*, 2001; 2(8): 675–80
46. Honda K, Sakaguchi S, Nakajima C et al: Selective contribution of IFN- $\alpha/\beta$  signaling to the maturation of dendritic cells induced by double-stranded RNA or viral infection. *Proc Natl Acad Sci USA*, 2003; 100(19): 10872–77